

Autumn and Winter Extreme Precipitation Events and their Relationship with ENSO, NAO and MJO Phases over the West of Iran

Jamshidi Khezeli, T.¹, Ranjbar Saadat Abadi, A.^{2*}, Nasr-Esfahany, M. A.³, Tajbakhsh Mosalman, S.⁴ and Mohebalhojeh, A. R.⁵

1. Ph.D. Student, Atmospheric Science and Meteorological Research Center (ASMERC), Tehran, Iran

2. Associate Professor, Department of Weather Hazards Warning, Atmospheric Science and Meteorological Research Center (ASMERC), Tehran, Iran

3. Assistant Professor, Department of Water Engineering, Shahrekord University, Shahrekord, Iran

4. Assistant Professor, Department of Atmospheric Prospecting, Atmospheric Science and Meteorological Research Center (ASMERC), Tehran, Iran

5. Professor, Department of Space Physics, Institute of Geophysics, University of Tehran, Tehran, Iran

(Received: 11 Jan 2021, Accepted: 20 Sep 2021)

Abstract

Some extreme precipitations have occurred in Iran in recent years. This paper is devoted to the study of extreme precipitations in the west of Iran, affected by combination of atmospheric pressure patterns in the period of 1987–2016. At first, monthly precipitations for seven synoptic stations of the west of Iran in autumn and winter with positive anomalies greater than 100% were identified. Then, for statistical-dynamical analysis, the El-Nino Southern Oscillation (ENSO), North Atlantic Oscillation (NAO), Madden-Julian Oscillation (MJO) indices were used. Results showed that the extreme precipitations had occurred during moderate to strong El-Nino, while MJO was critical and strong, in phases 2 and 8, and NAO was in positive phase. The anomalies of the MJO index in case studies had positive values. The NAO for case studies has entered a positive phase from a strong negative phase a few days before extreme precipitation. Analyzing the relationship between the NAO and the MJO with lagged composites showed when the MJO leads the NAO, significant positive NAOs are found for phases 2, and negative NAOs for phases 8, indicating a significant influence of the MJO on NAO. The synoptic-dynamic analysis showed that three low pressure and one high pressure were the dominant systems that have been effective in producing extreme precipitation. Examination of the moisture fluxes revealed that the main humidity sources of the heavy precipitation were the Arabian Sea due to easterly winds that travel a long distance over the north west of Indian Ocean to the Arabian Sea.

Keywords: Extreme precipitation, Pressure patterns, ENSO, MJO, NAO, West of Iran.

1. Introduction

An extreme weather phenomenon is an event that is significantly different from normal weather at a specific location and time. Extreme precipitation events can lead to flooding, mudslides and other damaging events. In recent years, heavy precipitation events have resulted in several damaging floods in the west of Iran. Two factors that can affect precipitation in the mountainous region of the west of Iran in the cold half of year are teleconnections and large scale rain bearing systems (Ahmadi Givi et al., 2009). The El-Nino Southern Oscillation (ENSO), Madden Julian Oscillation (MJO), and the North Atlantic Oscillation (NAO) are among the major teleconnections that impact different areas in the Northern Hemisphere on annual, intra-seasonal and monthly time scales respectively (Zhang et al., 2018;

Perdigon-Morales et al., 2019; Masato et al., 2013). The ENSO is the cycle of warm and cold sea surface temperature (SST) of the tropical central and eastern Pacific Ocean. It has been reported that ENSO events are accompanied by significant changes in the mid latitude Sea Surface Temperature (SST) patterns in the North Pacific and North Atlantic (Lau and Nath, 2001). El-Nino is accompanied by high pressure in the western Pacific and low pressure in the eastern Pacific. Each phase of ENSO is known to last on average about four years; however, records demonstrate that the cycles have also lasted between two and seven years. During the development of El-Nino, rainfall develops between September and November in the United States (Changnon, 2000). Many studies have shown that ENSO impacts on

*Corresponding author:

aranjbar@gmail.com

the precipitation in Iran and other areas (Tartaglione et al., 2003; Pagano et al., 2003; Nazemosadat and Ghasemi., 2004; Alizadeh-Choobari et al., 2018; Zhang et al., 2019; Nasuno, 2019; Takemi and Unuma., 2019; Dehghani et al., 2020).

The MJO with its eastward movement during the 30-60-day activity, affects the entire tropical region on an intra-seasonal scale and creates a strong convection zone on the Indian and Pacific oceans (Madden and Julian, 1971). The MJO through extreme changes in heating affects the subtropical atmospheric circulation by excitation of teleconnection patterns (Lau and Phillips, 1986; Knutson and Weickmann, 1987; Ferranti et al., 1990; Higgins and Mo, 1997; Matthews et al., 2004; Kamimera et al., 2012; Wu et al., 2013; Teng et al., 2019).

There is strong year-to-year (interannual) variability in MJO activity, with long periods of strong activity followed by periods in which the oscillation is weak or absent. Shimizu et al. (2016) analyzed the MJO influence on precipitation extreme events over the northern South America in El-Nino and La-Nina years. Extreme precipitation events over the northern South America for the rainy season (December–May) were obtained through a composite analysis of the combinations of ENSO and MJO phases. Most of the dry extreme events occurred during El-Nino periods, while wet extreme events were more recurrent during La-Nina or neutral years. They showed that the MJO convection could enhance or weaken the basic response of ENSO on extreme precipitation events. Moreover, the dry/wet extreme events over both Amazon and Northeast Brazil are favored when MJO convection over Indonesia is enhanced (MJO phases 4 and 5)/suppressed (MJO phase 2). Additionally, the interannual variability of the extreme events showed an increasing linear trend for the dry extreme events and a decreasing linear trend for the wet extreme events.

The NAO is also a large-scale meridional oscillation between the subpolar low-pressure system near Iceland and the subtropical anticyclone near the Azores area (Wallace and Gutzler, 1981; Barnston and Livezey, 1987). The positive phase of the NAO, due to the northward displacement of the North

Atlantic storms to higher latitudes, reduces the occurrence and severity of the cyclones to the west and center of the Mediterranean, but exerts less impact on the cyclones of the east of Mediterranean (Maheras et al., 2001; Alpert et al., 2004; Trigo et al., 2006; Nissen et al., 2010; Flocas, 2010; Corona and Montaldo, 2017; Wang et al., 2018).

An important component in the coherent fluctuations between the tropical medium-range variability and the extratropical circulation is the possible link between the MJO and the NAO. Numerous studies (e.g. Matsueda and Takaya, 2015; Henderson et al., 2016; Yadav and Straus, 2017; Lee et al., 2020) have been conducted on the relationship between MJO and NAO. Lin and Brunet (2008) showed the bivariate MJO index in the boreal winter seasons, significant connections between the NAO and the MJO are found. A prominent impact of the MJO on the North Atlantic localized NAO occurs after the MJO was observed in phases 2–4 and 6–8. When the MJO leads the NAO, significant positive NAOs were found for phases 2–4, and negative NAOs for phases 6–8, indicating a significant influence of the tropical MJO on the extratropical NAO variability. On average, the NAO index was positive 5 to 15 days after the MJO was detected in phases 2–4.

Cassou (2008) showed that daily maps of geopotential height led to four circulation patterns estimated from North Atlantic weather regimes extended boreal winter days. The probabilities of extreme events (cold outbreak, heavy rainfall) occurring were also related to the four weather patterns suggesting that a large part of the statistical distribution for surface variables, even regionally, could be assessed through the weather regime model.

With regard to the significant impact of the teleconnections on the increase of precipitation over the west of Iran in a short time period and specific locations, the behavior and effect of atmospheric teleconnections (including ENSO, MJO and NAO) on heavy precipitation during the past 30 years (1987-2016) are analyzed. The associated atmospheric circulations at different pressure level and anomaly patterns of geopotential height at 500 hPa are also identified. In addition, the relationship

between the MJO and the NAO on medium-range time scale and autumn and winter extreme precipitation events over the west of Iran are studied.

2. Methods and data

Initially, the monthly averaged value of precipitation accumulation at selected stations was compared with the long-term average of 30 years, and their anomalies were calculated.

The percentage values of anomaly are defined as:

$$\left(\frac{p-\bar{p}}{\bar{p}}\right) \times 100 \quad (1)$$

where p and \bar{p} are monthly precipitation and long-term monthly averaged values of precipitation, respectively (Bahrami et al., 2018). Then to investigate the teleconnection conditions, the indices of El-Nino, NAO and MJO were examined annually, monthly and daily, respectively.

The intensity of cold (warm) periods of the ENSO based on the Southern Oscillation Index (SOI) for the 30-years statistical period was classified (weak, moderate and strong). There are slight differences in the SOI values calculated at various centers. Here we used the SOI from CRU (Climate Research Unit), which is based on the method given by Ropelewski and Jones (1987). The SOI is a measure of the intensity or strength of the Walker Circulation. It is one of the key atmospheric indices for gauging the strength of El-Nino and La-Nina events. The SOI, defined as the normalized difference in surface pressure between Tahiti (French Polynesia) and Darwin in Australia, is a measure of the strength of the trade winds, which have a component of flow from regions of high to low pressure.

The months with anomalies greater than 100% (Laing, 2004) of precipitation and El-Nino episodes were investigated and monthly case studies were selected. In the following, for monthly case studies, the monthly values of NAO and SOI indices were checked and maximum daily precipitation as daily case studies were identified. For daily case studies, the behavior of the MJO (using Wheeler and Hendon (2004) daily diagrams) was investigated. The Wheeler-Hendon diagram is extremely useful in determining

the phase and amplitude of the MJO. For an MJO event to be considered active, the MJO index must be outside of the center circle of the diagram and show the evidence of an eastward propagation over the past days. Wheeler and Hendon (2004) introduced the pair of principal components that form the index of the real-time multivariate MJO series 1 (RMM1) and 2 (RMM2). RMM1 and RMM2 are dominated by the circulation components (Straub, 2013), nevertheless correlate highly with the MJO convective signal. Therefore, an index formed by RMM1 and RMM2 can be used to describe the evolution of the MJO. Principal Component Analysis (PCA) is a technique from statistics for simplifying a data set. PCA is a linear transformation that transforms the data to a new coordinate system such that the new set of variables, which are linear functions of the original variables, are uncorrelated, and the greatest variance by any projection of the data comes to lie on the first coordinate, the second greatest variance on the second coordinate, and so on (Jolliffe, 2002). When the MJO index for a certain period is greater than the average value of the total index in a phase, it is considered as a critical MJO (Alemzadeh et al., 2013).

According to the identified daily case studies, using the horizontal distribution of the mean sea level pressure, geopotential height and relative vorticity at 500 hPa level, relative humidity and vertical velocity at 700 hPa level, divergence of humidity flux at 925 hPa level, synoptic and dynamic conditions of atmospheric patterns and the combined systems were analyzed. A combined system is created when several independent pressure and precipitation patterns are merged together (Mohammadi et al., 2012).

In this study, the precipitation in the west of Iran including three provinces of Kermanshah, Lorestan and Ilam was considered (Figure 1). The quality controlled data of daily precipitation of autumn (October, November and December) and winter (January, February and March) from I.R. of Iran Meteorological Organization for seven synoptic weather stations have been used. To assess ENSO and NAO indices, as well as to identify the eight MJO phases, the datasets from the National Oceanic and

Atmospheric Administration (NOAA) and the Australian Meteorological data center have been used, respectively. ERA-Interim reanalysis data from the European Centre for Medium-Range Weather Forecasts (ECMWF) with a horizontal resolution of 0.75×0.75 degrees in longitude and latitude have been used to analyze the mean sea level pressure, geopotential height, wind field, relative humidity, humidity flux and vertical velocity at the pressure levels of 925, 700, 500 hPa.

3. Results and Discussion

3-1. The monthly averaged precipitation

In this section, the monthly averaged values of precipitation for the studied stations are compared to their long-term averaged values. In Figure 2, the blue horizontal line and red bar chart represent the long-term (30-years) and monthly averaged values of precipitation for the studied stations, respectively. According to Figure 2a-f, October 2015, February 2006, January 2004, November 1994, December 1991 and March 1987 had the highest monthly precipitation. Positive precipitation anomaly values in these months were about 462, 146, 75, 370, 122 and 195 percent, respectively. Preliminary statistical calculations showed that, except for January 2004, the monthly precipitation in October 2015, February 2006, November 1994, December 1991, and March 1987 had positive anomalies of higher than 100% relative to their long-term monthly averaged

values.

3-2. Investigating the status of teleconnections

3-2-1. ENSO events

The intensity of cold (warm) periods of the ENSO based on the SOI index (<http://www.bom.gov.au/climate/enso/enlist/>) for the 30-years period was investigated. In this period, the years of 1987, 1991, 1994, 1995, 1997, 2002, 2006 and 2015 experienced the El-Nino events and in the 1988, 1998 and 2011 the La-Nina events occurred. During the El-Nino period, the years of 1987, 1991, 1994 and 2015 were similar in intensity (moderate to strong).

3-3. Simultaneous study of maximum precipitation in the years of moderate to strong El-Nino

The investigation of ENSO events and the monthly averaged values of precipitation showed that the monthly averaged value of maximum precipitation with positive anomalies of above 100% occur in the years of moderate to strong El-Nino events. Figure 3 shows the monthly values of precipitation for the monthly case studies. According to Figure 3, the monthly values of precipitation accumulation in the west of Iran in November 1994, March 1987, October 2015 and December 1991 were about +4.6, +2.9, +5.5 and +2.2 times of the long-term monthly averaged value of precipitation, respectively.

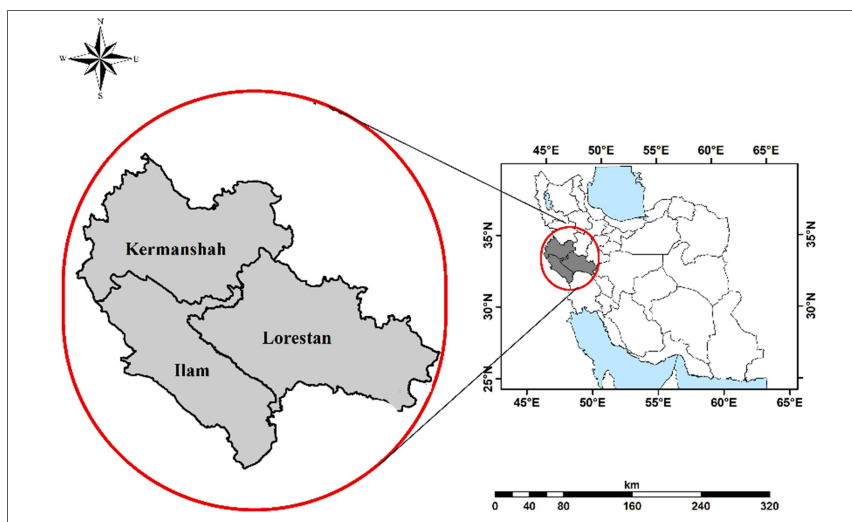


Figure 1. The location of the provinces in the west of Iran that have been studied.

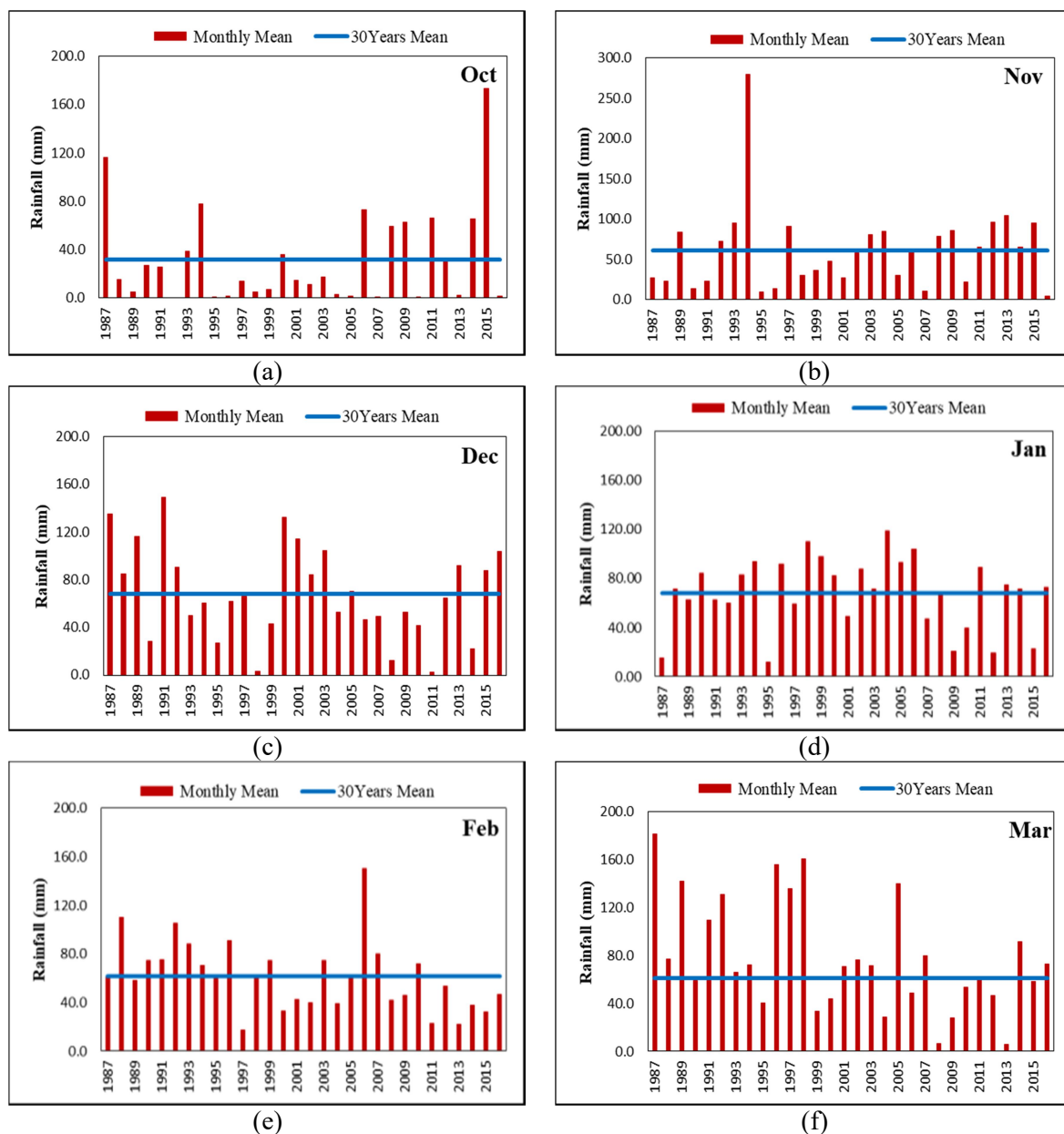


Figure 2. Monthly averaged (bar chart) and long-term averaged values (30-years) (blue line) of precipitation (mm). a-c and d-e show autumn and winter months, respectively.

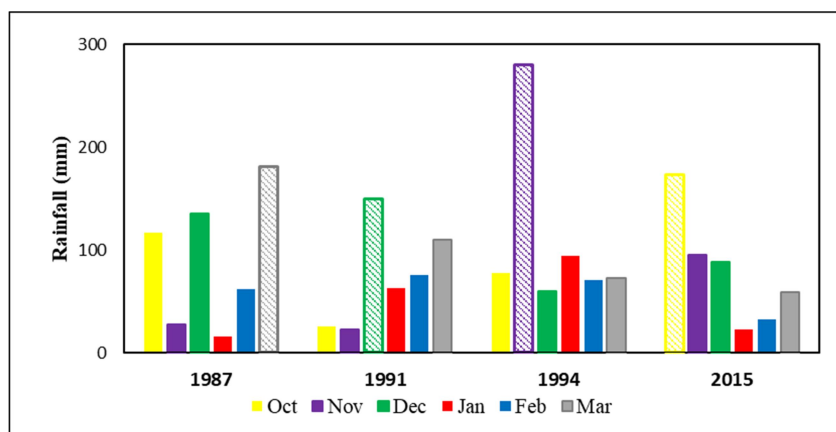


Figure 3. Monthly averaged value of precipitation (mm) of seven synoptic stations of the west of Iran in the El-Nino periods. The bars with diagonal lines are for the monthly case studies.

Figure 4 shows the isohyets map for Iran as a whole at the time of the moderate to strong El-Nino episodes in March 1987, December 1991, November 1994, and October 2015. In all the periods, most of the precipitation was concentrated in the western half, in particular, the west of Iran. According to the figures and isohyetal maps in the selected periods, the average values of precipitation in all stations of Iran in comparison to the long-term average have increased by about 57, 143, 70 and 111 percent in March 1987, December 1991, November 1994 and October 2015, respectively.

3-4. MJO and NAO

Table 1 shows days with maximum precipitation in the monthly case studies. Table 2 shows the long-term monthly averaged value of precipitation for the seven stations studied in the west of Iran, the daily value of maximum precipitation, as well as the status of teleconnections. The daily MJO index was in critical phase 8 in the case1 and case2 and critical phase 2 in the case3 and case4. The NAO index was also positive in all of monthly case studies.

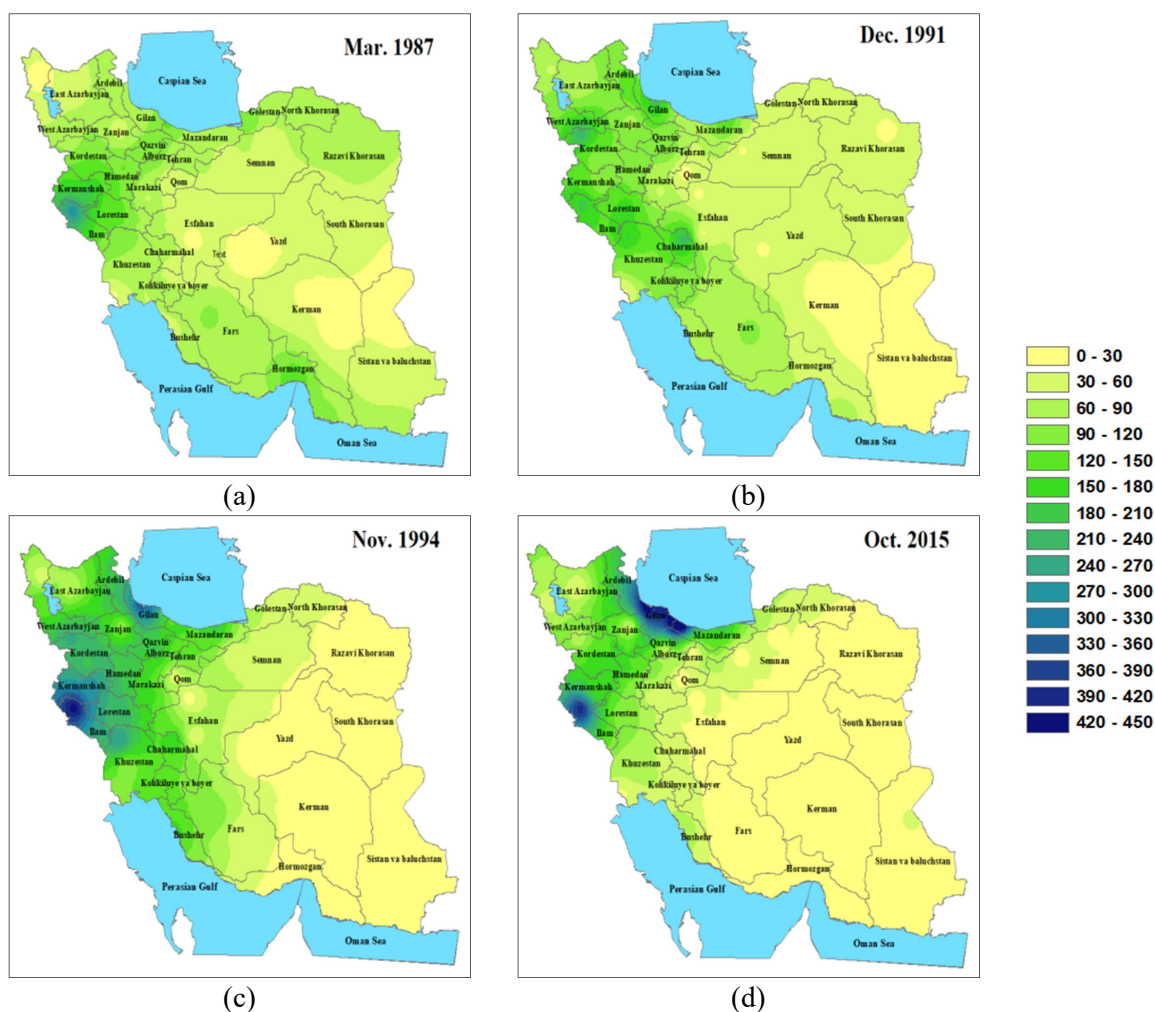


Figure 4. Isohyets (mm) maps in (a) March 1987, (b) December 1991, (c) November 1994 and (d) October 2015.

Table 1. Days of maximum precipitation in the case studies.

Year	Month	Day	Daily Case Studies
1987	Mar	3 th	Case1
1991	Dec	9 th	Case2
1994	Nov	21 th	Case3
2015	Oct	28 th	Case4

Table 2. Teleconnections status and precipitation values in the extreme precipitation periods in the west of Iran.

Daily Case Studies	Long-term Monthly average value of Precipitations (mm)	Daily Maximum Precipitation (mm)	El-Nino	MJO Phase (daily)	NAO (Monthly)
Case1	75.0	50	Moderate to Strong	8	0.14
Case2	65.4	102	Moderate to Strong	8	0.46
Case3	57.8	103	Moderate to Strong	2	0.64
Case4	30.5	282	Moderate to Strong	2	0.43

Figure 5 shows the annual variation of monthly average value of precipitation of the selected stations and the behavior of the three teleconnections. Figure 5-a illustrates the monthly averaged value of precipitation in the west of Iran, the SOI index, and the NAO index in 1987 and Figure 5-b presents the corresponds daily values of the MJO index in a 90-day interval. An investigation of the SOI changes from February to March shows that the index has been stronger in March (stronger El-Nino) than on February, and at the same time, the increase of precipitation in March in the western stations of the country has been higher than that of February. The MJO index has been in phases 6-8 from mid-February to maximum precipitation day, and its intensity has been rising to 1.9 on the 3rd and 4th day of March. It is noteworthy that most days from February to March 5th the MJO has been in phases 6-8 (this may be one of the factors contributing to the heavy precipitation conditions for the west of Iran (Ranjbar Saadatabadi and Soori, 2016). The NAO index has also been in the negative and strong phase on mid-February, which then turned into positive on March 1st.

According to Figure 5-c and Figure 5-d, the maximum precipitation has occurred in December 1991 in the seven stations studied. The MJO index was in the phase 8 with magnitude of about 2.1 during these three days. In this month, the monthly NAO index was positive and the SOI was about -17 (SOI intensity and precipitation values in December were higher than those in November).

According to Figure 5-e and Figure 5-f, the monthly average value of precipitation of the stations in November 1994 has been higher than the cases of March 1987 and December 1991. The maximum precipitation in this month was the highest value for the west of Iran in the studied statistical period. The

daily maximum precipitation was 103 mm on the 23rd day when the MJO was in phase 2 and entering phase 3 (Figure 5-f), the MJO index was about one unit weaker than those in 1987 and 1991. The NAO index was also positive and the SOI was about -7. In this month, the MJO and SOI indices were weaker than those in 1987 and 1991.

Figure 5-g and Figure 5-h show common condition of atmosphere for the case October 2015. The reported precipitation value in 29th October was 282 mm. A difference between the monthly precipitation of October 2015 with March 1987, December 1991 and November 1994 is that the maximum precipitation of October 2015 occurred during only four days (27-31th), while in the other cases precipitation occurred on most days of the month. The status of teleconnections in October 2015 has been as follows. The monthly averaged value of NAO index was positive and about unity. The MJO index ranged in the phase 2 from 27th to 31st October and entering phase 3. The MJO index was 2.4 on the 27th day, which was more intense than in the other daily case studies. The SOI was also -20, which was stronger when compared to the years 1987, 1991, and 1994. The impact of MJO on the precipitation of the selected years is as follows. In the monthly and daily case studies, when the MJO is in phases 6 to 8, the precipitation in the western regions of Iran has a significant positive anomaly. Given that phase 8 of the MJO is located on the western half of the Pacific Ocean and spatially overlaps with El-Nino, this situation intensifies the associated convergence and emission of moisture flux to the northwestern Indian Ocean and the Middle East (Farajzadeh et al., 2013). The shift of the NAO phase from negative (February) to the positive in March has caused anomalies and an increase in the amplitude of the NAO, sending waves along the meridional direction

and strengthening the trough in the eastern Mediterranean. It seems that when the MJO is in phase 2, the warm phase of ENSO (El-Nino) strengthens the convection and displaces the moisture flux to the northwest

of the Indian Ocean, north of the Red Sea and Iran. The positive phase of NAO also strengthens the eastern Mediterranean trough in these conditions (Ahmadi Givi et al., 2013).

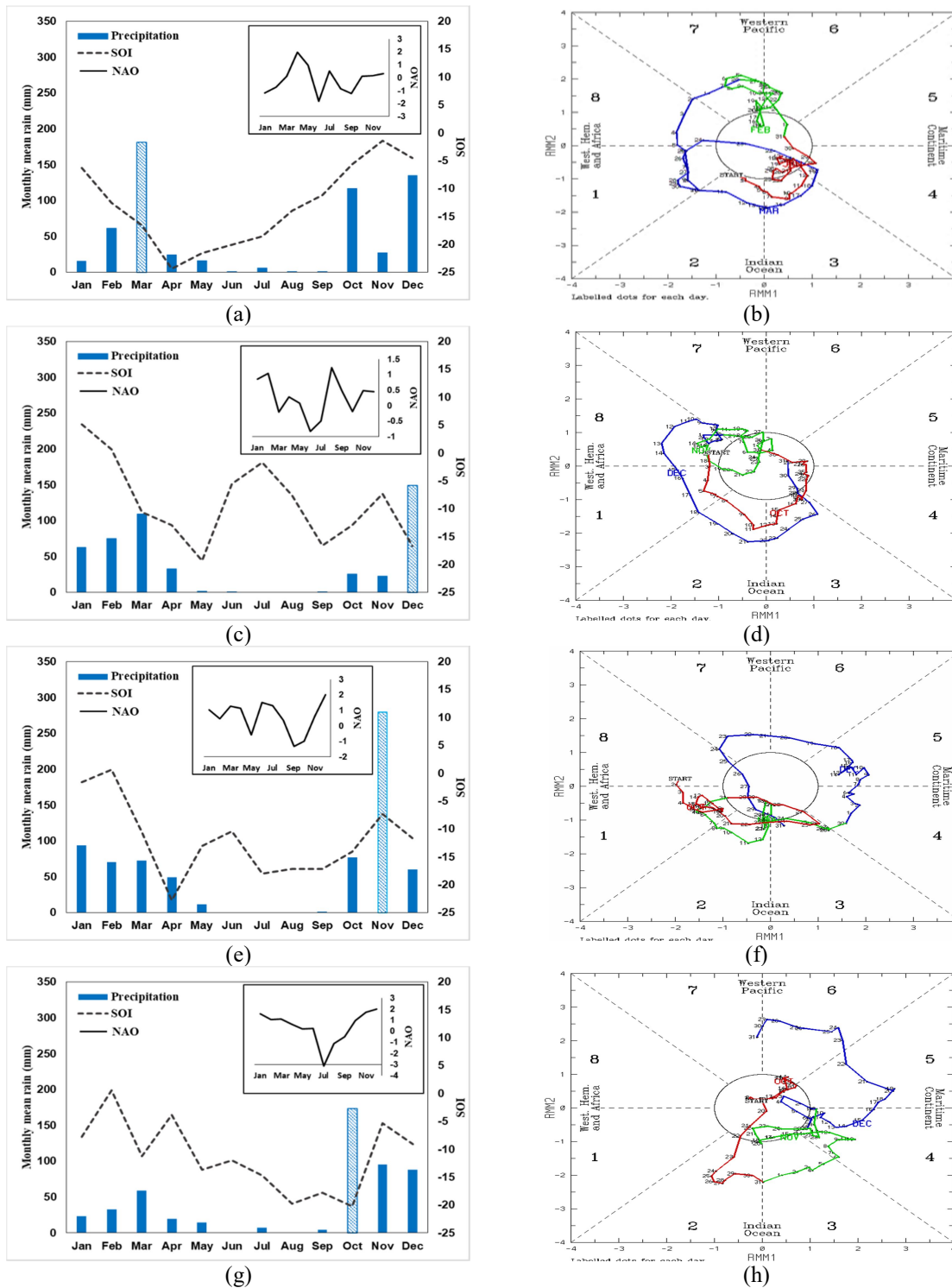


Figure 5. Monthly averaged values of precipitation (mm) variation in seven synoptic stations of the west of Iran and teleconnections behavior in (a), (b) 1987, (c), (d) 1991, (e), (f) 1994 and (g), (h) 2015 (diagonal lines show monthly case studies). In (d) 1991, (f) 1994 and (h) 2015, the red line is for October, the green line is for November and the blue line is for December. In (b) 1987, the red line is for January, the green line is for February and the blue line is for March.

3-4-1. MJO variations and anomalies

The MJO and NAO variation and their phases for the case studies have been shown at Table 3. The phases and daily values of MJO and NAO indices investigated from 15 days before to 3 days after the occurrence of extreme precipitation in four case studies in the statistical period. P and A indicate the phase and amplitude of MJO and N is the daily value of NAO index. Daily values greater than 1 for the MJO index have considered as critical values (Lin and Brunet, 2008; Cassou, 2008). In case 1 (C1) and case 2 (C2), the MJO was in phases 6-8 and underwent an increase in amplitude from 15 days before. The daily NAO index has entered a positive phase from a strong negative phase a few days before extreme precipitation. In case 3 (C3), MJO was in critical phases 2 and 3 from 13 to 7 days before and its range has decreased, and it has been strengthened again from two days before the extreme precipitation in phase 2. Also, from negative values, the NAO has entered a positive phase with an increasing trend. In case 4 (C4), MJO index from seven days before in phase 2 has been associated with an increase in amplitude. The NAO

index has been in a positive phase until the day of extreme precipitation.

Table 4 shows the anomaly of the MJO index in four case studies in the statistical period 1987-2016. According to Table 4, the anomaly of the MJO index in all four cases had positive values and the highest and lowest values were related to cases 4 and 3, respectively, with values of about 76% and 9%.

3-4-2. Relationship Between MJO and NAO

To analyze the connection between the NAO and the MJO, lagged composites are calculated for the NAO index for different phases (2 and 8) of the MJO, which are presented in Table 5. Positive lag means that the NAO lags the MJO of the specific phase, while for negative lag it is the NAO that leads the MJO. When the MJO leads the NAO, significant positive NAOs are found for phase 2, and negative NAOs for phase 8 (bold numbers), indicating a significant influence of the MJO on NAO. The NAO index is positive 5–15 days after the MJO is detected in phase 2 (bold numbers).

Table 3. MJO characteristics (P and A are phase and amplitude, respectively) and NAO index (N) for lag -15 to +3 days for four case studies (C1 to C4).

Day	-15	-14	-13	-12	-11	-10	-9	-8	-7	-6	-5	-4	-3	-2	-1	0	+1	+2	+3	
C1	P	7	7	7	7	7	6	6	6	6	6	7	7	7	8	8	8	8	1	
	A	0.7	0.9	1.1	1.4	1.1	1.2	1.4	1.6	1.7	1.8	1.8	1.9	2.0	2.0	2.0	1.9	1.9	1.8	1.7
	N	-0.4	-0.6	-0.7	-0.7	-0.9	-1.4	-1.5	-1.6	-1.7	-1.5	-0.9	-0.3	0.0	0.2	0.4	0.4	0.6	0.8	0.8
C2	P	7	7	7	7	7	7	8	8	8	8	8	8	8	7	8	8	8	8	
	A	0.3	0.3	0.8	1.0	0.9	1.1	1.3	1.6	1.6	1.4	1.3	1.2	1.2	1.5	1.6	1.9	2.0	2.1	2.3
	N	0.3	0.2	0.7	1.2	1.4	1.1	0.7	-0.5	-0.5	-0.9	-1.5	-1.2	-0.2	0.4	0.5	0.0	0.0	0.3	0.4
C3	P	1	1	2	2	2	2	2	2	2	3	3	2	2	2	2	2	2	3	
	A	1.6	1.6	1.7	1.6	1.6	1.7	1.6	1.2	1.0	0.9	0.8	0.5	0.4	0.4	0.9	1.3	1.3	1.0	1.0
	N	0.0	-0.1	-0.3	-0.8	-1.1	-1.2	-0.7	-0.3	0.1	0.4	0.3	0.2	0.4	1.0	1.3	1.0	0.9	0.8	0.3
C4	P	6	6	6	6	6	7	3	2	2	2	2	2	2	2	2	2	2	3	
	A	1.0	1.1	1.0	0.8	0.4	0.3	0.2	0.1	0.6	0.9	1.6	2.1	2.3	2.4	2.4	2.3	2.0	2.0	2.2
	N	0.4	0.6	0.7	0.6	0.5	0.5	0.7	1.1	1.4	1.3	0.8	0.8	0.6	0.2	0.0	-0.3	-0.7	-0.1	1.0

Table 4. MJO Anomaly in case studies during 1987-2016.

Case studies	Phase	Long-Term Monthly Average	Daily Amplitude	Anomaly (%)
Case1	8	1.46	1.90	29.86
Case2	8	1.24	1.86	49.74
Case3	2	1.15	1.25	9.08
Case4	2	1.29	2.28	76.09

Table 5. Lagged composites of the NAO index with respect to each MJO phase. Positive lag means that the NAO lags the MJO of the specific phase, while negative lag represents that the NAO leads the MJO

Case study	Case 1	Case 2	Case 3	Case 4
Phase	8	8	2	2
Lag -15	-0.8	0.1	0	0.7
Lag -10	-0.8	-0.2	0.2	0.8
Lag -5	-0.1	-0.4	0.6	0.5
Lag 0	0.4	0	1	-0.3
Lag 5	0.6	0.2	0.6	0.2
Lag 10	0.4	0.5	0.7	0.3
Lag 15	0.3	0.8	0.9	0.3

3-5. Large-scale weather conditions

This section synoptically and dynamically investigates the conditions of occurring heavy precipitation in the west of the country, with the anomalies greater than 100% compared to the long-term averaged values.

3-5-1. 500 hPa level

The 500 hPa maps (Figure 6) of 1987, 1991, 1994 and 2015 show that the trough and ridge (the blue and the red dashed line, respectively) are located on the eastern

Mediterranean and eastern Iran, respectively. Although these troughs have differences in term of intensity, but in October 2015, when the highest amounts of precipitation have occurred in the west of Iran, the intensity of trough has been about 100-200 gpm weaker than the other cases. For the 2015 case, the values of vorticity located ahead of the trough on the eastern Mediterranean have been around 0.5-1.5 ($10^{-5} s^{-1}$), which is almost the lowest amount among the cases studied.

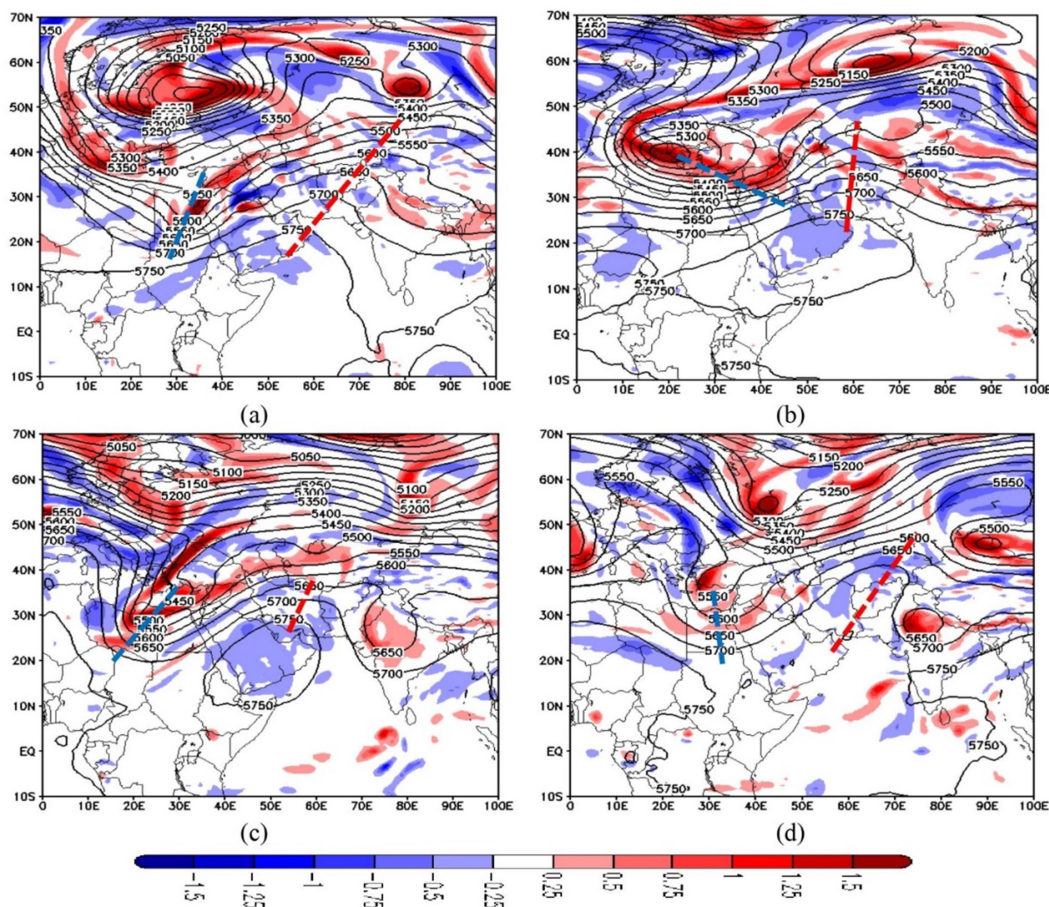


Figure 6. Geopotential height (gpm) and relative vorticity ($10^{-5} s^{-1}$) of 500 hPa level on 1200 UTC in (a) 03 March 1987, (b) 09 December 1991, (c) 21 November 1994 and (d) 28 October 2015. The blue and the red dashed line show the trough and ridge axes.

3-5-2. 1000 hPa level

Figure 7 shows the mean sea level pressure (MSLP) maps in the case studies. Investigation of large-scale atmospheric circulation in the case studies show the activity of low pressures located on the northwestern Indian Ocean (L1), the Sudan (L2) and the eastern Mediterranean (L3) with pressure ridge in eastern Iran (H) (Figure 7). The main differences between these systems are in the extension of the affected area and intensity of the L3 system such that there are strong low-pressure (L3) with 995-1000mb in March 1987 and December 1991, 1005 mb

in November 1994 and 1010 mb in October 2015. The low-pressure systems (L1, L2 and L3) and high-pressure system (H) have been present in all cases. The reason for the high precipitation occurrence in 2015 seems to be the extent of the low pressure (L1) over the part of Indian Ocean and the Arabian Sea, leading to the injection of significant moisture to the west of Iran by the cyclonic circulation and transfer over a long distance over the sea areas, despite the fact that the intensity of Mediterranean low pressure in this year is about 15-50 mb less than the other years studied.

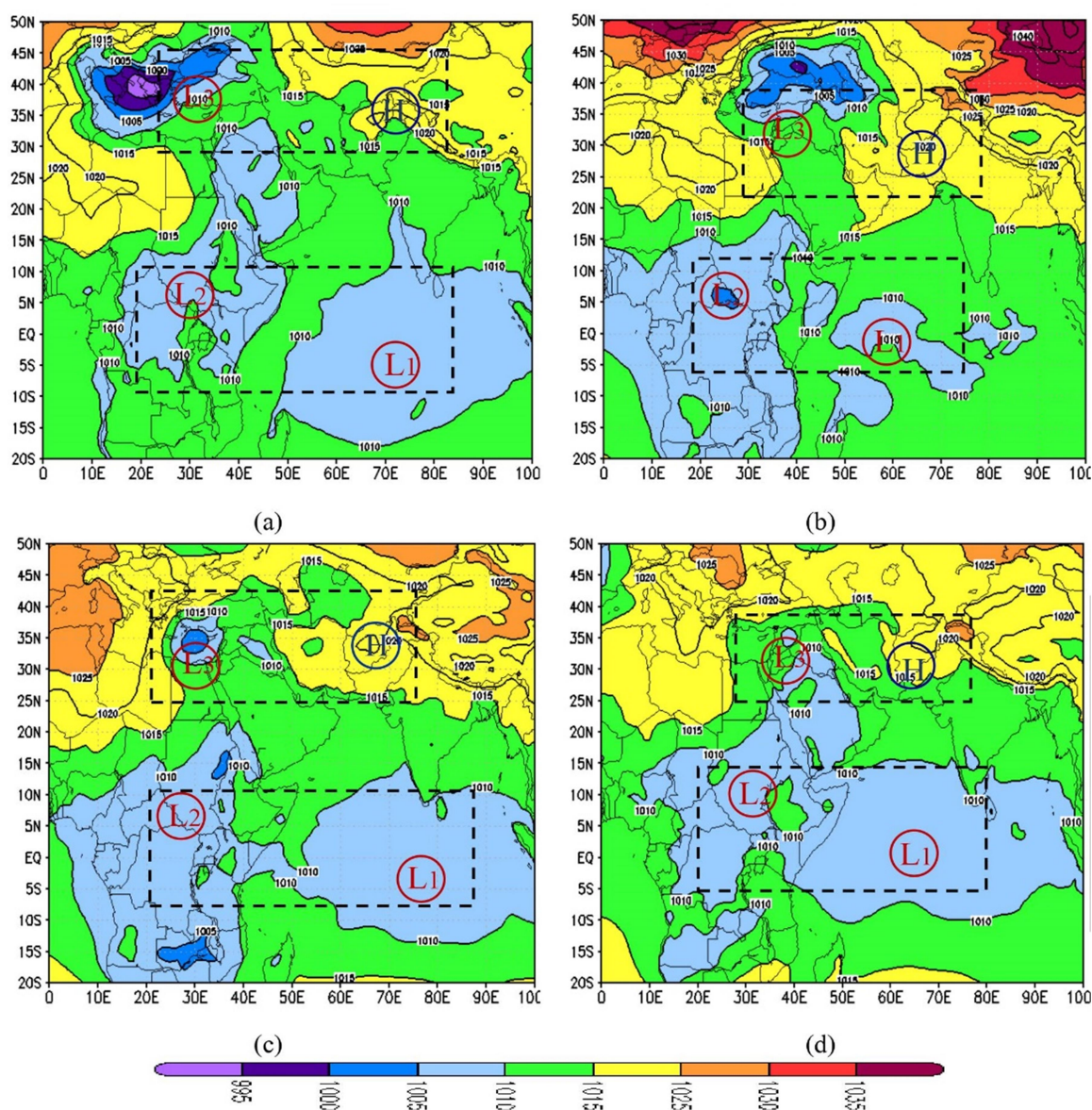


Figure 7. Mean sea level pressure (hPa) (a) on March 03, 1987, (b) December 09, 1991, (c) November 21, 1994 and (d) October 27, 2015. The dashed boxes show two system pairs.

3-5-3. 925 hPa level

Source and sink areas of moisture are presented based on the maps of divergence of moisture flux and humidity vector at 925 hPa level (Figure 8) with the red color representing the divergence of moisture flux and the green color is the corresponding convergence. In all the maps, there are two cyclonic centers over the Indian Ocean located in (65°E, 05°S) and (42°E, 03°S) and one cyclonic center over the north of Indian Ocean (60°E, 12°N). The wind field generated by the opposite motion of these two centers acted as strong sources of moisture makes the moisture flux transmitted by the anticyclonic center located in the southern regions of Iran

(60°E, 25°N) driven to south and southwest of Iran parallel to 25°N. The Indian Ocean and the Oman Sea have the cyclonic and anticyclonic centers and act as driving forces to transfer moisture over the Red Sea and the Persian Gulf to the western parts of Iran. In 1987 and 2015, in addition to the southern regions mentioned, the amount of moisture transferred from the Mediterranean to the west of Iran was considerable. The convergence of humidity flux associated with the cyclonic center (65°E, 5°S) in 2015 is stronger than that in other years. The amount of transferred moisture due to the wind field convergence in 1991 was lower than that in other years.

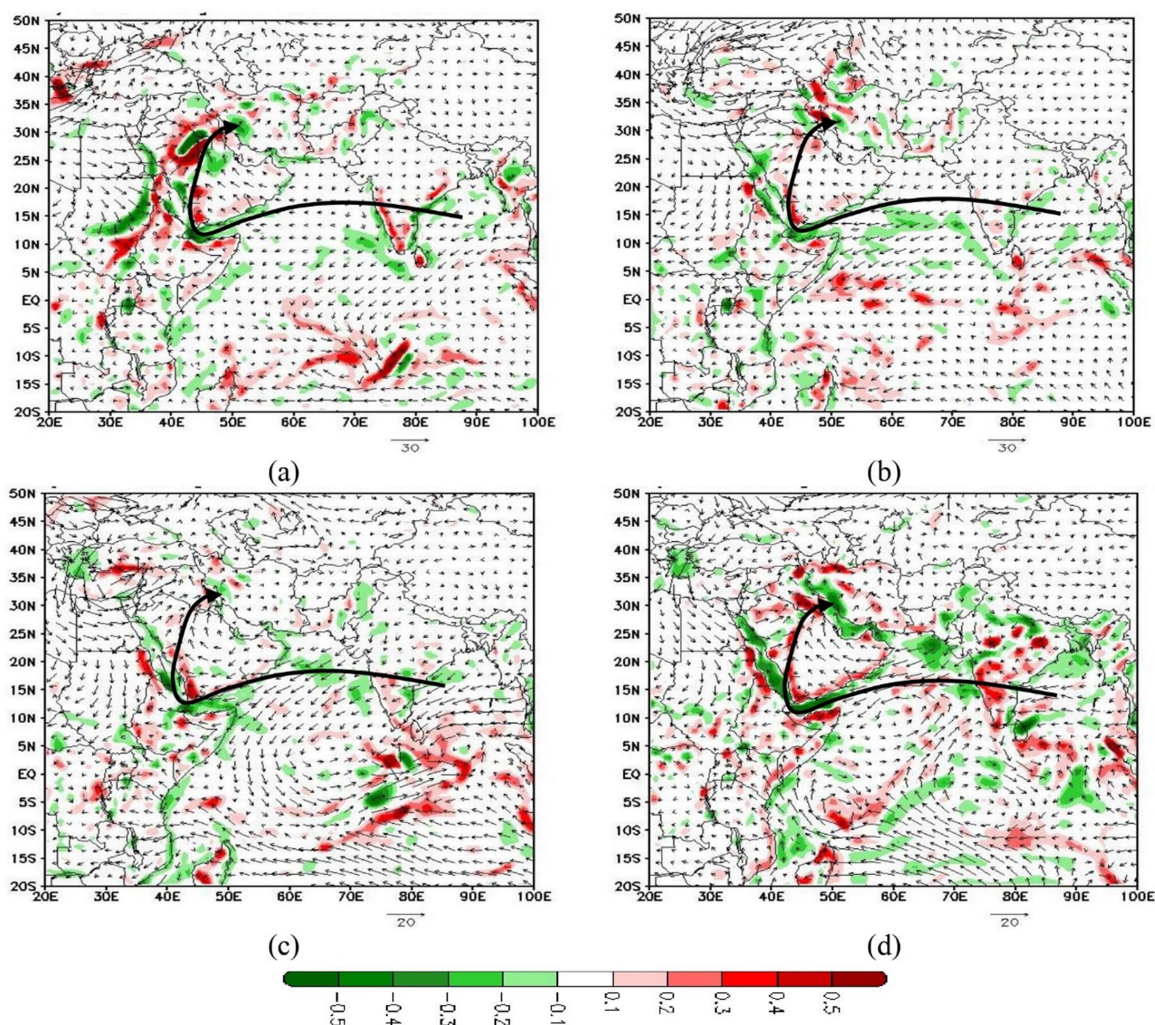


Figure 8. Flow and moisture flux divergence ($\text{kg m}^{-1} \text{s}^{-1}$) on March 03, 1987, (b) December 09, 1991, (c) November 21, 1994 and (d) October 28, 2015 at 925 hPa Level. Curved lines show the moisture transfer tracks.

3.5.4. Anomaly pattern of at 500 hPa

Investigation of geopotential height anomalies at 500 hPa for four case studies (Figure 9-a) showed that simultaneously with the negative height anomaly formed in the north Atlantic, a significant negative anomaly extended from western Russia to northern Sudan, the Red Sea and the western regions of Iran. Also, two positive anomaly centers are located on the North Atlantic and north of Europe, which is similar to the classic pattern of the Scandinavian blocking (Cassou, 2008), and eastern of Iran, respectively. This arrangement of anomalies leads to the occurrence of precipitation with positive anomalies greater than 100% in western Iran (Figure 9-b).

3-5-5. Anomaly pattern at 500hPa for lag -15, -10 and -5 days

Figure 10 shows the anomaly and mean values of geopotential height at 500 hPa based on 5-day mean during 15 days before

the occurrence of extreme precipitation for four case studies. Examination of geopotential height anomaly at 500 hPa showed that from 15 days before extreme precipitation, there have been two positive height anomaly with ridge over Europe and eastern Iran, and up to five days before extreme precipitation, the ridge located over Europe was weakened and a deep trough has been reinforced instead. Also, from 15 days before the occurrence of extreme precipitation, in the eastern Mediterranean with the cold air falling from the northern latitudes, the conditions are such that the trough (ridge) has been strengthened (weakened).

The significant positive geopotential height anomaly at 500 hPa over European (Scandinavian region) is shown to occur during MJO phases 6-8 (Henderson et al., 2016). In case 1 and case 2 associated with MJO phases 6-8 for lags of -15 to 0 days, positive geopotential height anomalies have been observed.

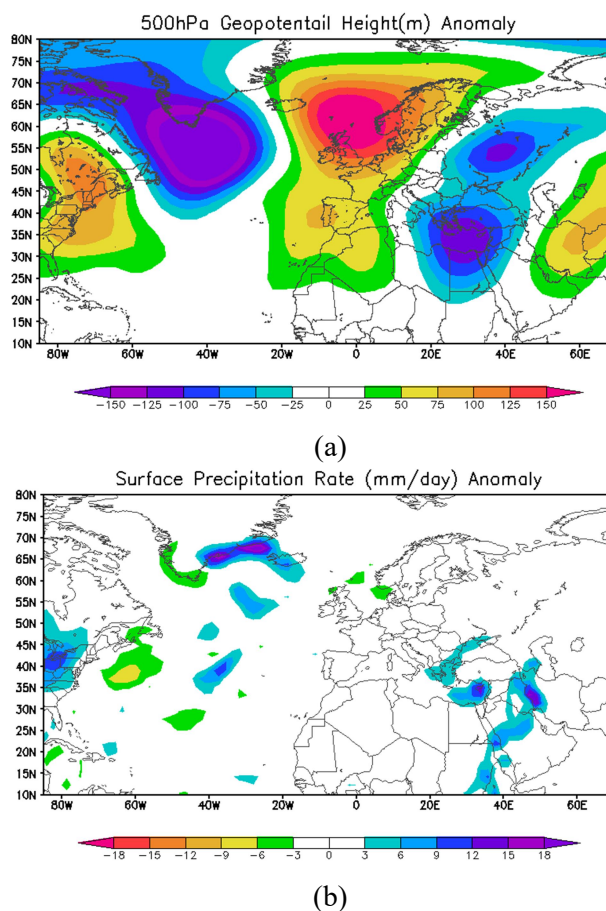


Figure 9. a) The geopotential height anomaly at the 500-hPa, b) Precipitation rate anomaly for four case studies.

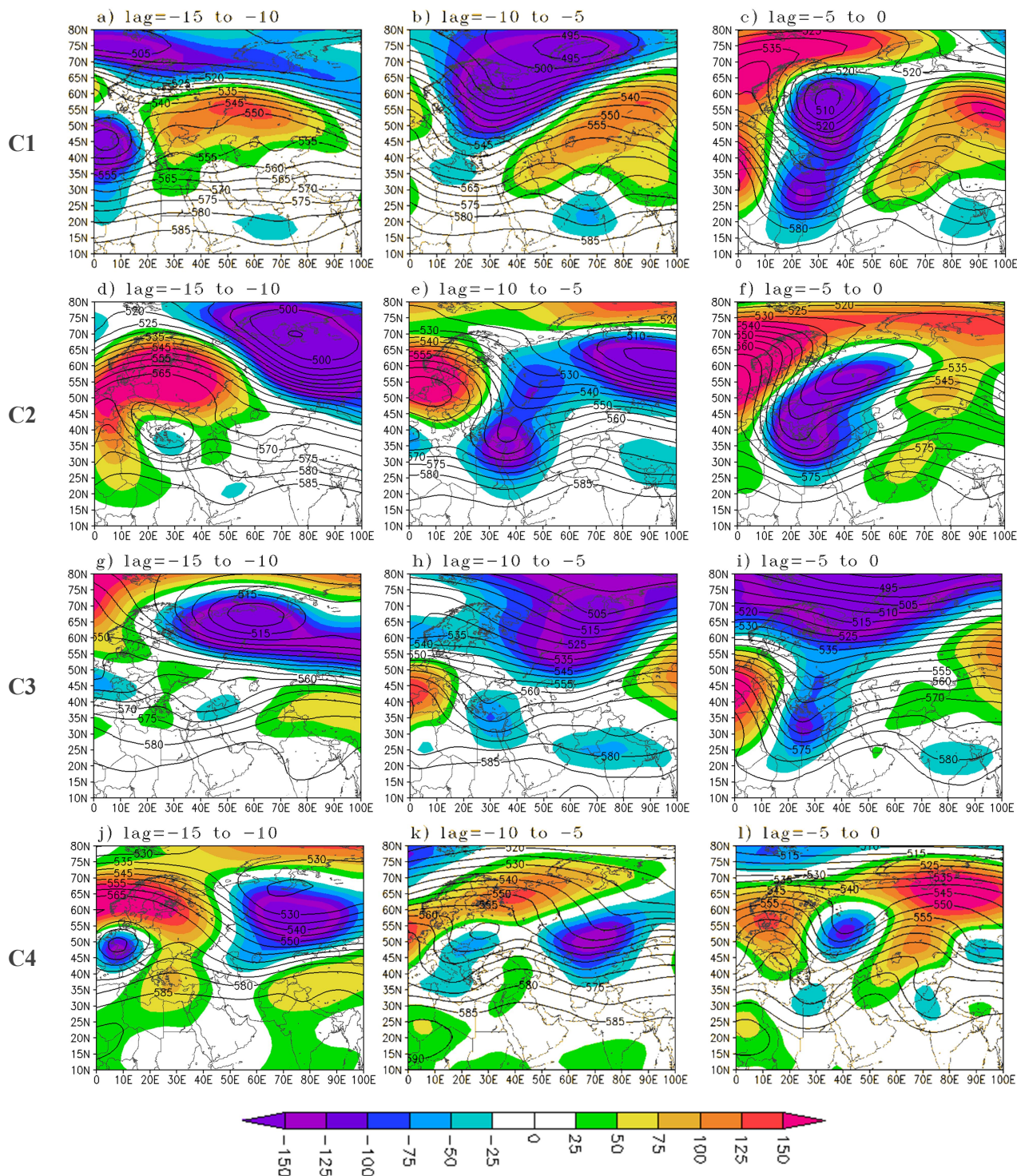


Figure 10. 500 hPa geopotential height anomalies for pentad 0, 1 and 2, where a pentad denotes a 5-day mean. Pentad 0 is the field average of days -5 to 0. (from left to right), (a, b, c), (d, e, f), (g, h, i) and (j, k, l) are for case 1 (3 Mar 1987), case 2 (9 Dec 1991), case 3 (21 Nov 1994) and case 4 (28 Oct 2015), respectively.

4. Conclusion

This study has investigated the effects of ENSO, MJO and NAO on the autumn–winter extreme precipitation on the west of Iran for the period of 1987–2016. The results showed that the precipitation anomalies were greater than +100 percent only for four months

(March 1987, December 1991, November 1994 and October 2015). These extreme precipitation anomalies have occurred in autumn and the last months of winter and did not occur in January and February. Therefore, there has been no precipitation such anomalies in January and February

associated with moderate to strong El-Nino events. In such cases of extreme anomalous precipitation, monthly precipitation values have increased throughout Iran from 57% (March 1987) to 143% (December 1991). The normalized precipitation anomalies (more than +100%) have occurred only in the warm phase of ENSO (El-Nino), where El-Nino and NAO were moderate to strong and positive, respectively. In the daily case studies, the MJO was in the critical phases 2 and 8. In addition, the results showed that before the occurrence of heavy precipitation over the studied area, the SOI was weak in January and February and for the heavy autumn precipitation events, SOI had strongly negative values in the April (November 1994) or May (December 1991). Investigation of MJO index variations revealed that the daily heavy precipitation events were associated with an increase of MJO index values and that MJO reached the critical phases 2 and 8 a few days before. Further, the occurrence of the highest value of MJO index coincided with the day of maximum precipitation.

The anomaly of the MJO index in all four case studies had positive values and the highest and lowest values were related to case 4 and case 3, respectively, with precipitation anomalies of about 76% and 9% greater than normal. In case 1 and case 2, associated with MJO index in phases 6-8, an increase of amplitude from 15 days before has been observed. In case 3, MJO was in critical phases 2 and 3 from 13 to 7 days before, then it has been strengthened from two days before the extreme precipitation. In case 4, the MJO index from seven days before in phase 2 has been associated with an increase in amplitude. The daily NAO index for four case studies has entered a positive phase from a strong negative phase a few days before extreme precipitation. Analyzing the relationship between the NAO and the MJO with lagged composites showed that when the MJO leads the NAO, significant positive NAOs are found for phase 2, and negative NAOs for phase 8, indicating a significant influence of the MJO on NAO. The NAO index is positive 5–15 days after the MJO is detected in phase 2. The results of the present study are in complete agreement with the results of Lin and Brunet (2008).

The synoptic-dynamic analysis showed that three low pressure and one high pressure systems were the dominant systems that have been effective in producing extreme precipitation. A pair of low pressure systems (L1 and L2) was active over the Indian Ocean and Sudan areas, respectively, and another pair of low–high pressure (L3 and H) was active over the eastern Mediterranean and some parts of Afghanistan–Pakistan areas, respectively. The Scandinavian blocking pattern leads to occurrence of precipitation with positive anomalies greater than 100% in western Iran. Examination of the moisture fluxes revealed that the main humidity sources of the heavy precipitation were the Arabian Sea due to easterly winds that travel a long distance over the north west of Indian Ocean to the Arabian Sea.

Investigating the variation of atmospheric teleconnection indices (SOI and NAO) revealed that all the cases of heavy precipitation had occurred when ENSO was in the warm phase (El Niño conditions) and often reached its maximum in the spring, and it underwent a reverse change in intensity from weakening to strengthening before the onset of extreme precipitation events. In the all cases, NAO was in the positive phase, and for the 1995 and 1996 cases before the heavy precipitation events, it changed from the negative to the positive. Our results point to a significant relationship between changes in these teleconnection indices and extreme precipitations in the west of Iran. As a final remark, further studies are suggested to find the underlying reasons for this connection from physical and dynamical points of view.

References

- Ahmadi Givi, F., Parhizkar, D. and Hajjam, S., 2009, The study of the ENSO's effect on the seasonal precipitation of Iran in the period 1971-2000, *Journal of the Earth and Space Physics*, 35, 95-113.
- Ahmadi-Givi, F., Nasr-Esfahany, M. and Mohebalhojeh, A. R., 2013, Interaction of North Atlantic baroclinic wave packets and the Mediterranean storm track, *Quarterly journal of the Royal Meteorology Society*, 140, 754-765.
- Alemzadeh, S., Ahmadi-Givi, F., Mohebalhojeh, A.R and Nasr-Esfahani, M.A., 2013, Statistical-dynamical analysis

- of the mutual effects of NAO and MJO, *Iranian Journal of Geophysics*, 7(4), 64-80.
- Alizadeh-Choobari, O., Adibi, P. and Irannejad, P., 2018, Impact of the El Niño–Southern Oscillation on the climate of Iran using ERA-Interim data, *Clim Dyn*, 51, 2897–2911.
- Alpert, P., Ziv, B. and Shafir, H., 2004, Semi-objective classification for daily synoptic systems: Application to the eastern Mediterranean climate change, *International Journal of Climatology*, 24(8), 1001-1011.
- Barnston, AG. and Livezey, RE., 1987, Classification, seasonality and persistence of low-frequency atmospheric circulation patterns, *Monthly Weather Review*, 115(6), 1083-1126.
- Bahrami, F., Ranjbar, A., Meshkatee, A.H. and Kamali, G.A., 2018, Study of the Atlantic and Mediterranean storm track based on Rassbi wave activity flux in the dry and wet periods of spring 2018 and 2008 in Iran, *Journal of Meteorology and Atmospheric Science*, 1,1-12.
- Cassou, C., 2008, Intraseasonal interaction between the Madden–Julian Oscillation and the North Atlantic Oscillation, *Nature*, 455, 523-527.
- Changnon, Stanley A., 2000, *El Niño 1997-98 The Climate Event of the Century*, New York: Oxford University Press, pp. 35. ISBN 0-19-513552-0.
- Corona, R. and Montaldo, N., 2017, On the Role of NAO-Driven Interannual Variability in Rainfall Seasonality on Water Resources and Hydrologic Design in a Typical Mediterranean Basin, *Journal of Hydrometeorology*, 19, 485-498.
- Dehghani, M., Salehi, S., Mosavi, A., Nabipour, N., Shamshirband, S. and Ghamisi, P., 2020, Spatial Analysis of Seasonal Precipitation over Iran: Co-Variation with Climate Indices, *ISPRS Int. J. Geo-Inf*, 9, 73.
- Farajzadeh, M., Ahmadi, M., Alijani, B., Qavidel Rahimi, Y., Mofidi, A. and Babaeian, I., 2013, Study on Variation of Major Teleconnection Patterns (MTP) associated with Iran's Precipitation, *Journal of Climate Research*, 15, 31-45.
- Ferranti, L., Palmer, TN., Molteni, F. and Klinker, E., 1990, Tropical-extratropical interaction associated with the 30–60-day oscillation and its impact on medium and extended range prediction, *Journal of the Atmospheric Sciences*, 47(18), 2177-2199.
- Flocas, HA., 2010, On cyclonic tracks over the eastern Mediterranean, *Journal of Climate*, 23(19), 5243-5257.
- Henderson, SA., Maloney, ED. and Barnes, EA., 2016, The Influence of the Madden–Julian Oscillation on Northern Hemisphere Winter Blocking, *Journal of Climate*, 29, 4597-4616.
- Higgins, RW. and Mo, KC., 1997, Persistent North Pacific circulation anomalies and the tropical intraseasonal oscillation, *Journal of Climate*, 10(2), 223-244.
- Jolliffe, IT., 2002, *Principal Component Analysis*, second edition, New York, Springer-Verlag New York.
- Kamimera, H., Mori, S., Yamanaka, M. D. and Syamsudin, F., 2012, Modulation of Diurnal Rainfall Cycle by the Madden–Julian Oscillation Based on One-Year Continuous Observations with a Meteorological Radar in West Sumatera, *SOLA*, 8, 111-114.
- Knutson, TR. and Weickmann, KM., 1987, 30–60 day atmospheric oscillations: Composite life cycles of convection and circulation anomalies, *Monthly Weather Review*, 115(7), 1407-1436.
- Lau, KM. and Phillips, TJ., 1986, Coherent fluctuations of extratropical geopotential height and tropical convection in intraseasonal time scales, *Journal of the Atmospheric Sciences*, 43(11), 1164-1181.
- Lau, N. and Nath, M. J., 2001, Impact of ENSO on SST variability in the North Pacific and North Atlantic: Seasonal dependence and role of extratropical sea–air coupling, *J. Climate*, 14, 2846–2866.
- Laing, AG., 2004, Cases of heavy precipitation and flash floods in the Caribbean during El-Niño winters, *Journal of Hydrometeorology*, 5(4), 577-594.
- Lee, JCK., Lee, RW., Woolniugh, SJ. and Boxall, LJ., 2020, The links between the Madden-Julian Oscillation and European weather regimes, *Theoretical and Applied Climatology*, 141, 567–586.
- Lin, H. and Brunet, G., 2008, An observed

- connection between the North Atlantic Oscillation and the Madden-Julian Oscillation, *Journal of Climate*, 22, 364-380.
- Madden, RA. and Julian, PR., 1971, Detection of a 40-50-day oscillation in the zonal wind in the tropical Pacific, *Journal of the Atmospheric Sciences*, 28(5), 702-708.
- Maheras, P., Flocas, HA., Patrikas, I. and Anagnostopoulou, CHR., 2001, A 40-year objective climatology of surface cyclones in the Mediterranean region: spatial and temporal distribution, *International Journal of Climatology*, 21(1), 109-130.
- Matthews, A. J., Hoskins, B. J. and Masutani, M., 2004, The global response to tropical heating in the Madden-Julian oscillation during Northern winter, *Quart. J. Roy. Meteor. Soc.*, 130, 1991-2011.
- Matsueda, S. and Takaya, Y., 2015, The global influence of the Madden-Julian oscillation on extreme temperature events, *J Clim*, 28(10), 4141-4151.
- Masato, G., Hoskins, B. and Woollong, T., 2013, Winter and summer Northern Hemisphere blocking in CMIP5 models, *Journal of Climate*, 26, 7044-7059.
- Mohammadi, H., Fattahi, E., Shamsipour, A.A. and Akabari, M., 2012, Dynamic analysis of Sudanese systems and heavy precipitation in southwestern of Iran, *Journal of Applied Researches in Geographical Sciences*, 24, 7-24.
- Nasuno, T., 2019, Moisture Transport over the Western Maritime Continent during the 2015 and 2017 YMC Sumatra Campaigns in Global Cloud-System-Resolving Simulations, *SOLA*, 15, 99-106.
- Nazemosadat, M. J. and Ghasemi, A. R., 2004, Quantifying the ENSO-Related Shifts in the Intensity and Probability of Drought and Wet Periods in Iran, *Journal of climate*, 17, 4005-4018.
- Nissen, K., Leckebusch, GC., Pinto, JG., Ulbrich, S. and Ulbrich, U., 2010, Cyclones causing wind storms in the Mediterranean: characteristics, trends and links to large-scale patterns, *Natural Hazards and Earth System Science*, 10(7), 1379-1391.
- Pagano, TC., Mahani, SH., Nazemosadat, MJ. and Sorooshian, S., 2003, Review of Middle Eastern hydroclimatology and seasonal teleconnections, *Iran J. Sci. Technol*, 27, 95-109.
- Perdigon-Morales, J., Romero-Centeno, R., Barrett, BS. and Ordonez, P., 2019, Intraseasonal variability of summer precipitation in Mexico: MJO Influence on the midsummer drought, *Journal of Climate*, 32(8), 2313-2327.
- Ropelewski, C.F. and Jones, P.D., 1987, An extension of the Tahiti-Darwin Southern Oscillation Index, *Monthly Weather Review*, 115, 2161-2165.
- Ranjbar Saadatabadi, A. and Soori, M., 2016, A study of the impacts of the MJO on atmospheric circulations and winter precipitation in Iran, *Iranian Journal of Geophysics*, 11(1), 49-65.
- Straub, K.H. 2013, MJO Initiation in the real-time multivariate MJO index, *Journal of climate*, 26, 1130-1151.
- Shimizu, M.H., Ambrizzi, T. and Liebmann, B., 2016, Extreme precipitation events and their relationship with ENSO and MJO phases over northern South America, *International Journal of Climatology*, 37, 2977-2989.
- Tartaglione, CA., Smith, SR. and O'Brien, JJ., 2003, ENSO impact on hurricane landfall probabilities for the Caribbean, *J. Climate*, 17, 2925-2931.
- Takemi, T. and Unuma, T., 2019, Diagnosing Environmental Properties of the July 2018 Heavy Rainfall Event in Japan, *SOLA*, 15, 60-65.
- Trigo, R., Xoplaki, E., Zorita, E., Luterbacher, J., Krichak, S., Alpert, P., Jacobeit, J., Saenz, J., Fernandez, J., Gonzalez, F., Herrera, F., Rodo, X., Brunetti, M., Nanni, T., Maugeri, M., Turkws, M., Gimeno, L. and Ribera, P., 2006, Relations between variability in the Mediterranean region and mid-latitude variability, *Developments in Earth and Environmental Sciences*, 4, 179-226.
- Teng, KC., Malonet, E. and Barnes, E., 2019, The consistency of MJO teleconnection patterns: An explanation using linear Rossby wave theory, *Journal of Climate*, 32(2), 531-548.
- Wallace, J.M. and Gutzler, D.S., 1981, Teleconnections in the geopotential height field during the Northern Hemisphere winter, *Monthly Weather Review*, 109(4),

- 784-812.
- Wang, L., Li, T., Chen, L., Behera, S. K. and Nasuno, T., 2018a, Modulation of the MJO intensity over the equatorial western Pacific by two types of El Niño, *Climate Dyn*, 51, 687–700.
- Wheeler, M.C. and Hendon, H.H., 2004, An all-season real-time multivariate MJO index: development of an index for monitoring and prediction, *Monthly Weather Review*, 132, 1917-1932.
- Wu, Arbain, A. A., Mori, S., Hamada, J. I., Hattori, M., Syamsudin, F. and Yamanak, M. D., 2013, The Effects of an Active Phase of the Madden-Julian Oscillation on the Extreme Precipitation Event over Western Java Island in January 2013, *SOLA*, 9, 79-83.
- Yadav, P. and Straus, DM., 2017, Circulation response to fast and slow MJO episodes, *Mon Weather Rev*, 145(5), 1577–1596.
- Zhang, Q., Gu, X., Li, J., Shi, P. and Singh, V., 2018, The impact of tropical cyclones on extreme precipitation over coastal and inland areas of China and its association to ENSO, *Journal of Climate*, 31(5), 1865–1880.
- Zhang, P., Wand, B. and Wu, Z., 2019, Weak El-Nino and winter climate in the mid-to high latitudes of Eurasia, *Journal of Climate*, 32(2), 405-421.